Thermochimica Acta, 11 (1975) 79–88

FORMATION, DISSOCIATION AND EXPANSION BEHAVIOR OF PLATINUM GROUP METAL OXIDES (PdO, RuO_2, IrO_2)

G. BAYER

Institute for Crystallography and Petrography, Swiss Federal Institute of Technology, Zürich (Switzerland)

H. G. WIEDEMANN

Mettler Instrumente AG, Greifensee/Zürich (Switzerland)

(Received 12 September 1974)

ABSTRACT

The oxidation behavior of palladium, ruthenium and iridium powders of different grain sizes was investigated by TG, DTA and X-ray methods. The solid oxides formed during heating up (PdO, RuO_2, IrO_2) show different stability and decomposition temperatures depending on the oxygen pressure. The kinetics of the reaction $MeO_x \rightarrow Me + x/2\ O_2$ is discussed. High temperature X-ray studies confirmed the strong anisotropy of thermal expansion in the case of RuO_2 and IrO_2. The thermal expansion behavior of these oxides is compared to that of other rutile-type oxides.

INTRODUCTION

The oxidation behavior of platinum metals is of importance in applications at high temperatures, e.g., for heating element materials, for crucibles and linings in containers for melting special glasses or growing single crystals, for catalysts, and for electrodes. The thermodynamics and reaction kinetics in the systems platinum metal–oxygen have been studied extensively by various investigators[1–10]. The results showed that all of these metals form solid oxides and also volatilize as oxides at higher temperature in oxidizing atmosphere. Most of the gaseous oxides are stable only at high temperatures and usually contain the metal in its highest oxidation states. Palladium is an exception since it dissolves oxygen in the solid state and only forms the solid oxide PdO which dissociates at temperatures above 800 °C. The adherence, stability and thickness of solid oxide films formed on platinum metals during heating up depends on the thermal properties of the oxides including the vapor pressures of the oxides and also of the metals.

Figure 1 shows the position of the six platinum metals in the periodic system together with the thermodynamically well-characterized oxides. The crystal structures of the solid oxides have been determined[11]. PdO and PtO are isostructural and show

25 Mn	26 Fe	27 Co	28 Ni	29
43 Tc	44 Ru RuO_2 (s) RuO_3 (g) RuO_4 (g)	45 Rh Rh_2O_3 (s) RhO_2 (s)	46 Pd PdO (s)	47
75 Re	76 Os OsO_2 (s) OsO_3 (g) OsO_4 (s)	77 Ir IrO_2 (s) IrO_3 (g)	78 Pt PtO (s) Pt_3O_4 (s) PtO_2 (s)	79

Fig. 1. Oxides of platinum metals.

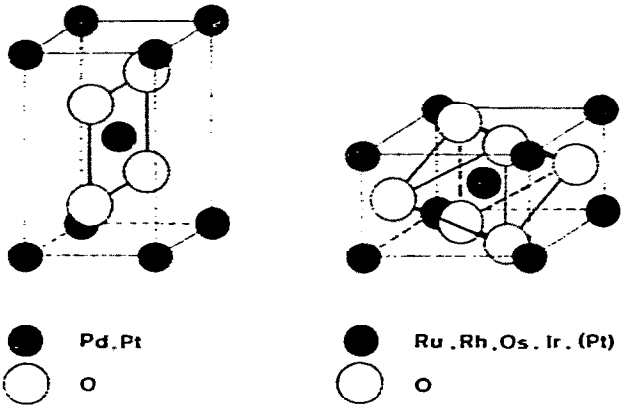

Fig. 2. Crystal structure of platinum metal oxides MeO and MeO_2.

the typical square, planar oxygen coordination (Fig. 2). Interesting is the predominance of the dioxides MeO_2[12,13] with rutile structure (Fig. 2), e.g., RuO_2, RhO_2 (high pressure form), OsO_2, IrO_2 and PtO_2 (high pressure form, orthorhombic distortion). Some of the solid oxides especially RuO_2, IrO_2 and PdO find increasing applications in thick film glaze resistors because of their high electrical conductivity over a wide temperature range. For such ceramic applications not only the thermal stability but also the thermal expansion of the oxides is of interest. The present investigations were concerned with the formation, stability and thermal expansion of PdO, RuO_2 and IrO_2. The results will be discussed in the following and are compared to other data reported in the literature.

EXPERIMENTAL

The platinum metals used in the experiments were catalyst powders (Heraeus) with specific surface areas of 10–30 $m^2 g^{-1}$ and purity >98% (difference due to adsorbed gases[14]). Oxides were prepared by heating the metal powders on thin alumina substrates for 2–4 days at 400–1000°C in air. Figure 3 shows a typical IrO_2-crystal grown during such heat treatment. The oxidation of metals and the decomposition of oxides were investigated with a Mettler thermoanalyzer which was

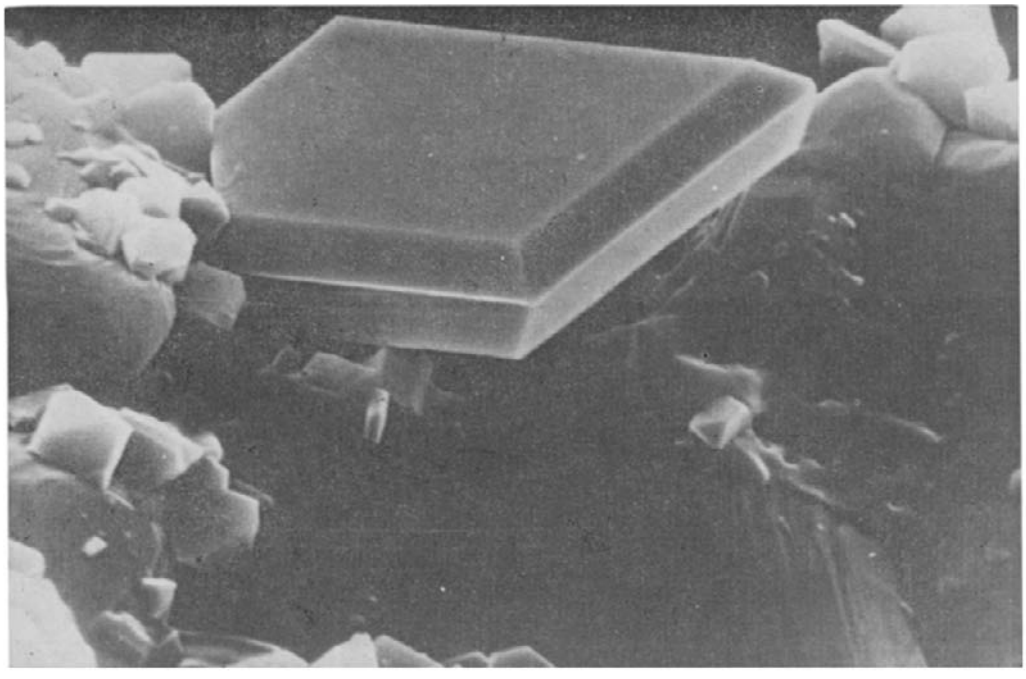

Fig. 3. Scanning electron micrograph of a IrO_2-crystal (11 625x).

combined with an Enraf nonius high temperature X-ray camera (System Lenné, CuK_α-radiation). Sample weights were in the order of 5–40 mg. TG and DTA curves were recorded under different atmospheric conditions (air, oxygen, vacuum) and with different heating rates and heating schedules. Stepwise heating over a longer period, e.g., holding the temperature constant for 1 h, then raising the temperature within 5 min by 1°C and so on, could be achieved by a combination of two electronic timers (one for preselecting the temperature interval, the other for switching on and off). Oxygen partial pressures were measured with a differential manometer within ±1 torr in the region 10–760 torr.

The thermal expansion of the oxides was determined by means of a high temperature X-ray diffractometer (MRC furnace, $CuK\alpha$-radiation). The 2θ region 40–100°C was scanned isothermally at the rate of 1 degree 2θ/4 min at 20, 220, 420, 750, 920 and 1020°C. Lattice constants were then calculated from two separate groups

of reflections. The accuracy and reproducibility of the linear thermal expansion coefficients were both better than $\pm 10\%$ relative. The precisely known axial thermal expansion of α-Al_2O_3 was used for checking the alignment of the instrument. The temperature of the Pt–Rh heating strip was calibrated with melting-point standards from Merck, with LiCl, NaCl and Na_2SO_4 to $\pm 10°C$ at the highest temperature.

RESULTS AND DISCUSSION

Figure 4 and Table 1 show results on the formation and dissociation of the oxides PdO, RuO_2 and IrO_2. The TG curves were obtained under reduced oxygen pressure (100 torr) and heating rates of $10°C\ min^{-1}$. The assignment of reaction

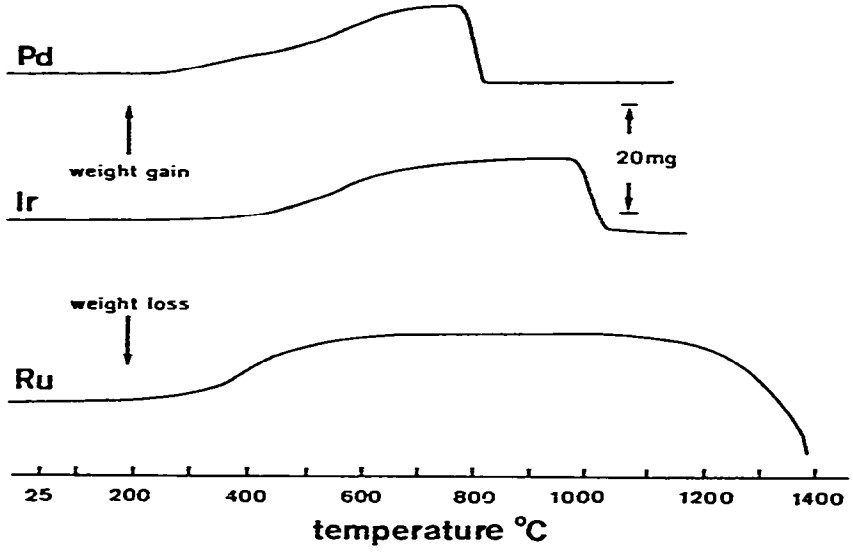

Fig. 4. Formation and dissociation of PdO, IrO_2 and RuO_2 at $P_{O_2} = 100$ torr. TG curves, heating rate $10°C\ min^{-1}$, sample weights 50–100 mg.

TABLE 1

FORMATION AND DISSOCIATION TEMPERATURES OF PdO, IrO_2 AND RuO_2

Oxygen pressure 100 torr, heating rate $10°C\ min^{-1}$.

Starting material	*Oxidation temp. (°C)*			*Dissociation temp. (°C)*		
	T_i	$T_{max.}$	T_e	T_i	$T_{max.}$	T_e
Pd-black,	196 (1)	567	664 (1)	762 (1)	806	819 (1)
8.5 $m^2\ g^{-1}$	258 (2)		740 (2)	775 (2)		828 (2)
Ir-black,	142 (1)	560	685 (1)	945 (1)	1005	1031[a] (1)
21.2 $m^2\ g^{-1}$	408 (2)		907 (2)	975 (2)		—
Ru-black,	118 (1)	405	500 (1)	928 (1)	1490	—
17.0 $m^2\ g^{-1}$	312 (2)		698 (2)	1438 (2)		—

[a] Temperature influenced by simultaneous vaporization.

temperatures was carried out according to Fig. 5. It was found that the formation and dissociation of the oxides depend on the oxygen pressure, on the heating rate and on the surface area of the metal powders. Decrease of oxygen pressure also favored the complete oxidation of the metal powders, especially Ru and Ir, whereas high oxygen pressures build up a thick surface layer immediately which retards further oxidation. Figure 6 gives a detailed picture of the course of the reaction when heating palladium

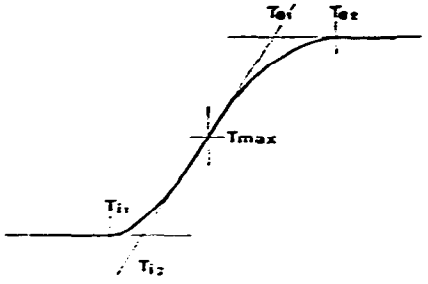

Fig. 5. Assignment of reaction temperatures in TG curves.

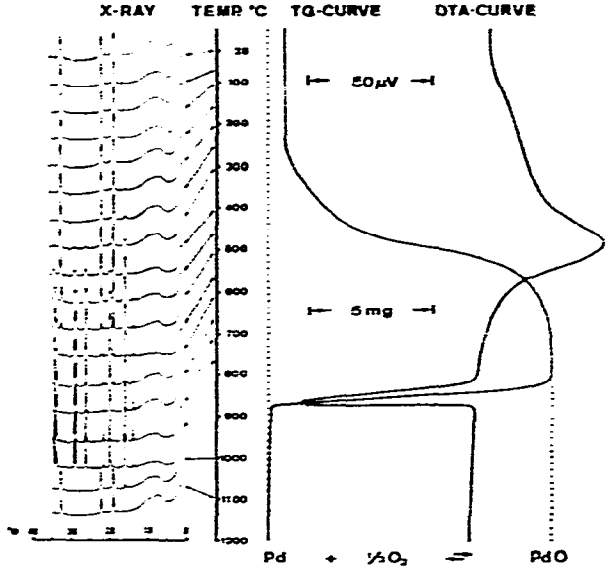

Fig. 6. Oxidation of palladium in air (5 l h^{-1}) and decomposition of PdO (sample weight 78 mg, heating rate 8°C min^{-1}).

in air. The TG curve, the DTA curve and the heating X-ray photograph (shown as photometric scan) were obtained simultaneously. The first traces of PdO can be seen already at 200°C, the oxidation is completed at about 700°C and dissociation takes place rapidly in the temperature range 820–850°C. These temperatures are influenced by the grain size of the metal, by the heating rate and atmosphere.

A series of experimental runs were carried out on the dissociation of PdO at oxygen pressures varying from 717 torr down to 10 torr. The dissociation temperature (T_{max}) of PdO decreases in this range from 872 °C at 717 torr down to 689 °C at 10 torr. A plot of these dissociation temperatures versus the equilibrium oxygen pressures is shown in Fig. 7 in the usual logarithmic form. The oxygen dissociation pressure reaches 1 atm at 877 °C. The heat of dissociation of PdO was calculated from the slope of the line

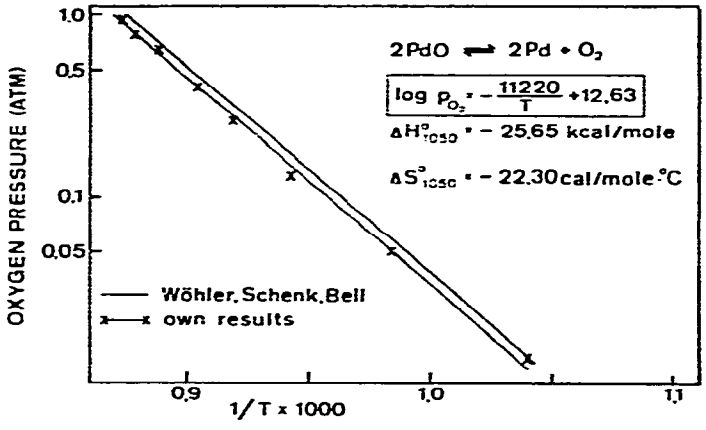

Fig. 7. Dissociation pressure of palladium oxide. ΔH and ΔS refer to 1 mole PdO.

by regression analysis. The medium temperature in the measured range was 777 °C = 1050 °K. Calculated values for $\Delta H^{\circ}_{1050} = -25.65 \pm 0.86$ kcal mol^{-1} and $\Delta S^{\circ}_{1050} = -22.30 \pm 0.77$ cal mol^{-1} °C^{-1} are in agreement with the data reported in the literature[15–17]. Using the heat capacity equation given by Kelley[18] $\Delta C_p = -6.08 + 12.32 \times 10^{-3} T + 0.20 \times 10^{5} T^{-2}$ it is possible to convert these values to the standard state: $\Delta H^{\circ}_{298} = -27.37$ kcal mol^{-1} and $\Delta S^{\circ}_{298} = -24.00$ cal mol^{-1} °C^{-1} for the reaction $PdO(s) \rightleftharpoons Pd(s) + 1/2 O_2$. These values correspond directly to the heat and entropy of formation of PdO from the elements. The relationship between equilibrium oxygen pressure and temperature which is given by the equation in Fig. 7, $\log p_{O_2} = -11{,}220/T + 12.63$, applies to $2PdO(s) \rightleftharpoons 2Pd(s) + O_2$. Therefore the molar values ΔH and ΔS correspond to half of the values derived from the slope of the line in Fig. 7. A comparison of the dissociation data of PdO to those reported for IrO_2

TABLE 2

DISSOCIATION DATA OF PdO, IrO_2 AND RuO_2

	ΔH°_{298} (*kcal mol^{-1}*)	ΔS°_{298} (*cal mol^{-1} °C^{-1}*)	$T_{diss.}$ (°C) ($p_{O_2} = 1$ *atm*)
PdO	−27.37	−24.00	877
IrO_2	−52.42	−40.52	1124
RuO_2	−71.17	−41.40	1580

and RuO_2[1-3] is given in Table 2. RuO_2 which has the closest packed structure also is the most stable oxide.

These measurements on the oxidation of palladium prove that it is possible to obtain thermodynamic data also by dynamic, thermoanalytical methods. The values compare favorably with those obtained by static, calorimetric methods. The slight discrepancies observed at present are due to the effect of the heating modes used in these measurements. A stepwise heating approaches more the isothermal conditions whereas a linear, even slow heating often is in advance of the actual reaction. Figure 8 shows schematically this effect on the position of T_i, T_{max}, T_e, and on the temperature interval, respectively.

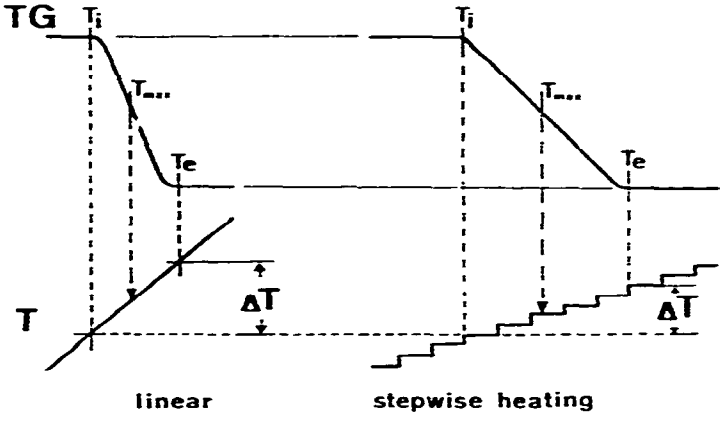

Fig. 8. Schematical presentation of the dependence of dissociation on the heating schedule. The dissociation temperatures used in Fig. 7 correspond to T_{max}.

Thermal expansion coefficients were calculated from the temperature dependence of lattice constants. Figures 9–11 show plots of the lattice constants a and c versus temperature for PdO, IrO_2 and RuO_2. The expansion coefficients are listed in Table 3 as average values over two temperature ranges. Palladium oxide shows medium, nearly isotropic expansion in agreement with its framework structure built up by interconnected PdO_4-squares. Actually the coordination is rectangular since the O–O distance is shorter in the z-direction (2.67 Å) than in the x- or y-direction (3.05 Å). This may contribute to the slightly larger expansion along c. IrO_2 and especially RuO_2 are characterized by a very strong expansion anisotropy. Compared to other compounds with rutile-structure they show reverse anisotropy, which means higher expansion in the a-direction and lower expansion in the c-direction (Table 4). RuO_2 is unique in this respect since it contracts in the c-direction during heating. This negative α_c is compensated by high expansion coefficients α_a in such a way that the volume expansion is similar to that of IrO_2. This unusual behavior of RuO_2 and to a lesser degree of IrO_2 cannot be explained simply by geometrical factors. Table 4 proves that there are no straightforward relationships between ionic radius, length of c-axis, c/a ratio or packing density (volume of oxygen atoms in the elementary

cell/volume of elementary cell) and the expansion coefficients along the c- or the a-axes. There is a general trend, however, that α_c is smaller for rutile compounds with larger c, that means increase of O–O distance in the z-direction[21]. MgF_2 is shown as comparison of a predominantly ionic rutile compound with lower valent ions to the rutile type oxides with varying ionic–covalent bond character. The more ionic the bond and the lower the valency the higher is generally the thermal expansion. The

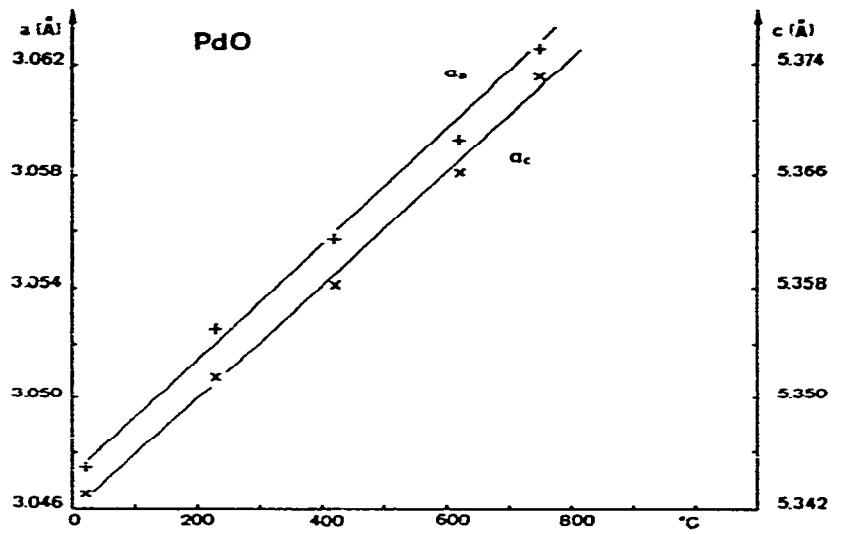

Fig. 9. Thermal expansion of PdO, changes of lattice constants a and c with temperature.

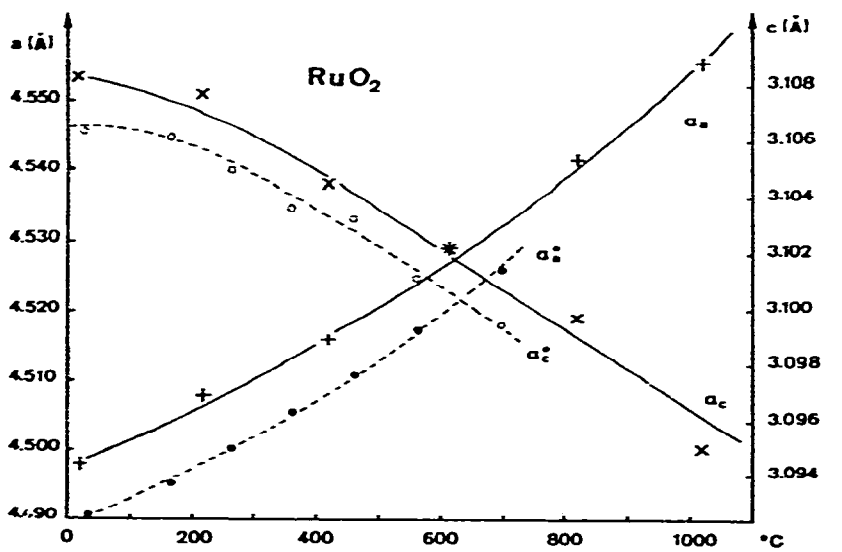

Fig. 10. Thermal expansion of RuO_2 compared to data reported in the literature (dashed lines, ref. 20).

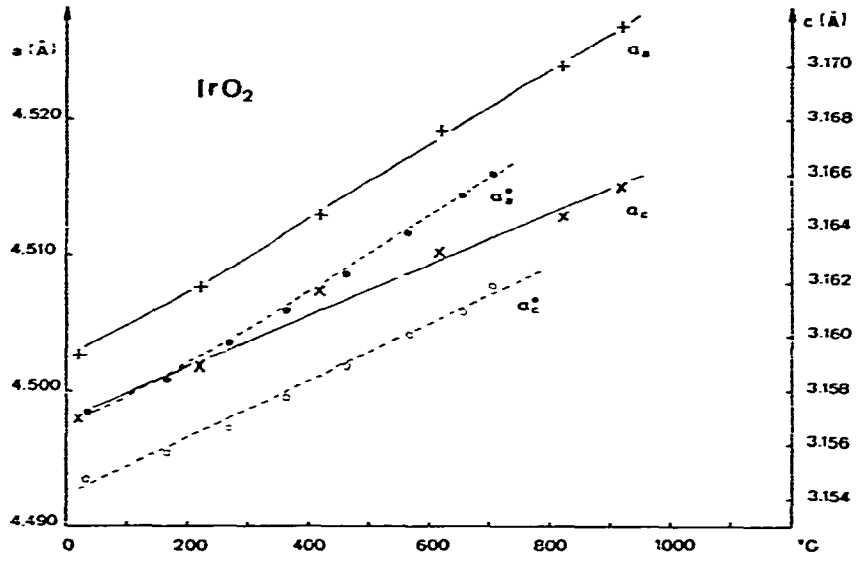

Fig. 11. Thermal expansion of IrO_2 compared to data reported in the literature (dashed lines, ref. 19).

special expansion characteristics of RuO_2—high α_a and negative α_c—were found also in the case of the rutiles CrO_2 and FeF_2[20]. All these compounds contain transition element ions with empty and half-filled d-orbitals. This could be of influence to certain Me–O bond directions and to the expansion in such directions.

TABLE 3

LATTICE CONSTANTS OF PdO, IrO_2 AND RuO_2 AT VARIOUS TEMPERATURES

Temp. (°C)	*PdO*		*IrO_2*		*RuO_2*	
	a(Å)	*c*(Å)	*a*(Å)	*c*(Å)	*a*(Å)	*c*(Å)
20	3.0475	5.3430	4.5026	3.1571	4.4980	3.1084
220	3.0525	5.3516	4.5075	3.1589	4.5079	3.1078
420	3.0557	5.3582	4.5124	3.1617	4.5164	3.1046
620	3.0593	5.3662	4.5192	3.1632	4.5294	3.1022
750	3.0625	5.3731	—	—	—	—
820	—	—	4.5241	3.1645	4.5416	3.0998
920	—	—	4.5272	3.1656	—	—
1020	—	—	—	—	4.5554	3.0950
T (°C)	20–420	20–750	20–420	20–920	20–420	20–1020
$\bar{\alpha}_a$[a]	6.7±0.4	6.7±0.5	5.5±0.3	6.1±0.4	10.2±0.8	12.7±0.9
$\bar{\alpha}_c$[a]	7.1±0.6	7.7±0.7	3.6±0.2	3.0±0.2	−3.1±0.3	−4.3±0.3

[a] $\bar{\alpha}_a$ and $\bar{\alpha}_c \times 10^{-6}$/°C.

TABLE 4

THERMAL EXPANSION OF RUTILE-TYPE COMPOUNDS

	Radius of cation (Å)	*Lattice constants (Å)*		*Packing density (%)*	*Linear thermal expansion (20–520°C, $\times 10^{-6}$/°C)*			
			c/a		α_a	α_c	α_a/α_c	$\bar{\alpha}$
TiO_2	0.61	$a = 4.5916$ $c = 2.9663$	0.646	74	7.8	9.6	1.23	8.4
SnO_2	0.69	4.7350 3.1843	0.673	64	4.3	5.0	1.16	4.5
RuO_2	0.62	4.4980 3.1084	0.691	73	10.2	−3.1	−0.30	5.8
IrO_2	0.63	4.5026 3.1571	0.701	72	5.5	3.6	0.65	4.8
MgF_2	0.72	4.6201 3.0511	0.660	61	12.9	18.0	1.40	14.6

ACKNOWLEDGMENTS

The authors acknowledge the assistance of E. Sturzenegger and H. D. Wiedemann.

REFERENCES

1 H. Schäfer and H. J. Heitland, *Z. Anorg. Allg. Chem.*, 304 (1960) 249.
2 H. Schäfer, W. Gerhardt and A. Tebben, *Z. Angew. Chem.*, 73 (1961) 27.
3 H. Schäfer, G. Schneidereit and W. Gerhardt, *Z. Anorg. Allg. Chem.*, 319 (1963) 327.
4 H. Schäfer, A. Tebben and W. Gerhardt, *Z. Anorg. Allg. Chem.*, 321 (1963) 41.
5 W. E. Bell, M. Tagami and R. E. Inyard, *J. Phys. Chem.*, 70 (1966) 2048.
6 J. C. Chaston, *Platinum Metals Rev.*, 8 (1964) 50.
7 J. C. Chaston, *Platinum Metals Rev.*, 9 (1965) 51.
8 C. L. McDaniel and S. J. Schneider, *J. Res. Nat. Bur. Stand.*, 73A (1969) 213.
9 D. Chatterji and R. W. Vest, *J. Amer. Ceram. Soc.*, 54 (1971) 73.
10 E. S. Ramakrishnan, *Script. Metall.*, 7 (1973) 305.
11 R. W. G. Wyckoff, *Crystal Structures*, Vol. 1, Interscience, New York, 2nd ed., 1965.
12 R. D. Shannon, *Solid State Common.*, 6 (1968) 139.
13 D. B. Rogers, R. D. Shannon, A. W. Sleight and J. L. Gillson, *Inorg. Chem.*, 8 (1969) 841.
14 R. Maurer and H. G. Wiedemann, *Thermal Analysis*, Vol. 1, *Proc. 2nd ICTA, Worcester, 1968*, 1969, p. 177.
15 L. Wöhler, *Z. Elektrochem.*, 11 (1905) 836.
16 R. Schenck and F. Kurzen, *Z. Anorg. Allg. Chem.*, 220 (1934) 97.
17 W. E. Bell, R. E. Inyard and M. Tagami, *J. Phys. Chem.*, 70 (1966) 3735.
18 K. K. Kelley, *Bur. Mines Bull. 584*, Washington, D.C., 1960.
19 K. V. Krishna Rao and L. Iyengar, *Curr. Sci.*, 38 (1969) 304.
20 K. V. Krishna Rao and L. Iyengar, *Acta Crystallogr.*, A 25 (1969) 302.
21 H. P. Kirchner, *J. Amer. Ceram. Soc.*, 52 (1969) 379.